THE JOURNAL OF PHYSICAL CHEMISTRY B

Article

pubs.acs.org/JPCB

External Heavy-Atomic Construction of Photosensitizer Nanoparticles for Enhanced in Vitro Photodynamic Therapy of Cancer

Lin Zhou,[†] Shaohua Wei,[†] Xuefeng Ge,[†] Jiahong Zhou,*[,†] Boyang Yu,*[,‡] and Jian Shen[†]

[†]Analysis and Testing Center, College of Chemistry and Materials Science, Jiangsu Key Laboratory Biofunctional Materials, Nanjing Normal University, Nanjing 210046, China

[‡]Department of Complex Prescription of TCM, China Pharmaceutical University, Nanjing 210038, China

Supporting Information

ABSTRACT: Introduction of heavy atoms around photosensitizers (PSs) generally facilitates intersystem crossing (ISC) and improves their quantum yield of singlet oxygen ($^1O_2$) generation ability, which is a key species in photodynamic therapy (PDT). Here, we report Pt(IV)- and Au(III)-modified silica nanoparticles (SN) as the drug delivery system of a hypocrellin A (HA) to improve its photodynamic activity through external heavy atom effect. Comparative studies with Pt- and Au-modified and unmodified nanoparticles have demonstrated that the intraparticle external heavy atom effect on the encapsulated HA molecules significantly enhances their efficiency of $^1O_2$ generation and, thereby, the in vitro photodynamic efficacy to cancer cells. The results well elucidated the potential of our PSs/heavy metal ions doped nanocarrier for improving the actual efficacy of PDT.

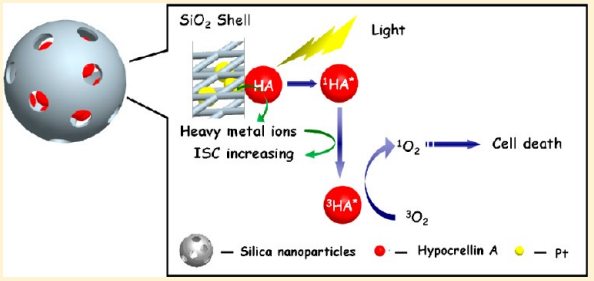

INTRODUCTION

Photodynamic therapy (PDT) is a potential tool in cancer treatment, based on the generation of reactive oxygen species (ROSs), especially $^1O_2$, by excitation of administered PSs with light. As a consequence of ROSs, cells undergo apoptosis or necrosis.[1−3] Hypocrellin A (HA) is an effective photosensitizer because of its high $^1O_2$ quantum yields. However, the hydrophobic nature limited its solubility in physiological condition, which hinders its system administration because HA tends to aggregate in blood plasma and block vascular networks.[4,5]

We have earlier used silica nanoparticles (SN) as delivery system of HA[6−9] because of their simple preparation processes, tunable size, easy modification, and compatibility in biological systems.[10] Systemic studies indicated that the resulting drug-doped nanoparticles are stable in aqueous system, can be active taken up by tumor cells, and have superior photoinduced anticancer activity to free HA. One possible way to further raise their photosensitization ability is to modulate the photophysical property of the encapsulated HA by introducing a certain intermolecular interaction to increase the $^1O_2$ generation efficacy.[11]

$^1O_2$ is generally considered to play the main role in PDT process. As shown in Scheme 1, $^1O_2$ is produced through the reaction between the long-lived triplet state of PS (^{3}PS*) and surrounding molecular oxygen. Irradiation with light elevates the electrons of PS to a higher energy level (^{1}PS*). Population of the ^{3}PS* occurs as a result of ISC from the photoexcited

Scheme 1. Simplified Jablonski Diagram for the PDT Process: (I) Absorption and (II) Fluorescence

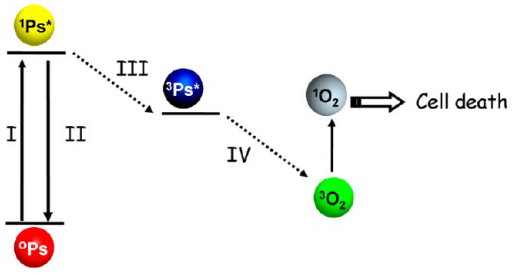

singlet PS (^{1}PS*), so the quantity of generated $^1O_2$ is dependent on the efficiency of ISC (^{1}PS* to ^{3}PS*). It is well-known that the rate of ISC can be increased as a result of enhanced spin−orbit coupling by the presence of heavy atoms. Enhanced spin−orbit perturbations can be achieved by the internal heavy atom effect (attachment of a heavy atom directly onto the molecule) or external heavy atom effect (placing the molecule in a surrounding environment containing heavy atoms).[12,13] Different from internal heavy atom effect, external heavy atom effect can effectively avoid reducing singlet-oxygen ability of PS caused by the structural distortions of the parent PS. This has been explained by the fact that the larger atomic

Received: May 27, 2012
Revised: September 10, 2012
Published: September 17, 2012

radii of the heavy atoms led to structural distortions of the parent PS, giving rise to loss of sensitizer planarity, which promoted nonradiative decay to the ground state and as a result a decrease in singlet-oxygen quantum yields.[14−19]

Reports indicated that introduction of heavy metal ions, such as Pd(II), Au(I), Au(III), Ag(III), Cu(III), or Pt(II), into a photosensitizer can improve their $^1O_2$ generation ability.[13−15,20−22] Besides, compared with using nonmetal heavy atoms, often iodine or bromine,[11,12] to modify the drug delivery carriers, using heavy metal provides more choices.[14] Furthermore, preparation of the metal ions modified ceramic materials has been well studied.[23,24] However, there is no research about using this technique for PSs delivery to improve their PDT efficiency. So, here, Pt(IV)- and Au(III)-modified SN were exploited as the carrier of HA. Comparative studies with Pt(IV)- and Au(III)-modified and unmodified SN have demonstrated that the intraparticle external heavy atom effect on the encapsulated HA molecules significantly enhances the efficiency of $^1O_2$ generation and, thereby, the in vitro PDT efficacy.

EXPERIMENT AND METHODS

3-Aminopropylmethyldiethoxysilane (APMDS) was from Acros. $H_2PtCl_6·6H_2O$, $HAuCl_4·4H_2O$, and 9,10-anthracenedipropionic acid were from Sigma. 3-[4,5-Dimethylthiazol-2-yl]-2,5-diphenyltetrazolium bromide (MTT) and Hoechst 33342 were from Amosco. Dulbecco's minimum essential medium (DMEM) and fetal calf serum (FCS) were from Gibico.

The Pt(IV)-doped HA encapsulated SN (Pt/SiO_2/HA) and Au(III)-doped HA encapsulated SN (Au/SiO_2/HA) were prepared as follows: 15 μL of HA (15 mM in DMF) was combined with 200 μL of APMDS and 20 mL of methanol. Subsequently, 200 μL of ammonia (28%) as the hydrolysis catalyst was added to the above mixture accompanied by vigorous magnetic stirring for 30 min. For Pt/SiO_2/HA, 23 μL (19.3 mM in methanol) of H_2PtCl_6 was added to the above system; for Au/SiO_2/HA, 10 μL (44.6 mM in methanol) of $HAuCl_4$ was added to the above system. The resulting solution was then kept under stirring at room temperature for 24 h. For HA-encapsulated SN (SiO_2/HA), H_2PtCl_6 or $HAuCl_4$ was not added. Samples were vacuum dried to remove methanol and then redissolved in water and dialyzed again water for 24 h, and our results indicated that no HA, Pt, or Au could be detected in the dialyzed water. The final molar ratio of HA and SiO_2 was about 1:4 of all of the particles, and the molar ratio of HA and Au (or Pt) was about 1:2 in the heavy atom modified SiO_2.

Transmission electron microscopy (TEM) was employed to determine the morphology and size of the aqueous dispersion, using a Hitachi H-7650 electron microscope, operating at an accelerating voltage of 120 kV. Ultraviolet−visible spectroscopy (UV−vis) absorption spectra were recorded using a Varian Cary 5000 spectrophotometer in a quartz cuvette with a 1 cm light path. Microscopy fluorescence images were acquired by an Axiovert 40 Carl Zeiss microscopy. Fluorescence spectra and fluorescence lifetime were obtained using a Horiba Jobin Yvon FM-4P-TCSPC system. The dynamic light scattering (DLS) was measured with Malvern Zetasizer Nano 90 measurements in aqueous systems.

$^1O_2$ generation was determined by the 9,10-anthracenedipropionic acid disodium salt (ADPA) bleaching method, taking HA as reference. ADPA is bleached by singlet oxygen to its corresponding endoperoxide ($ADPAO_2$) and the reaction was monitored spectrophotometrically by recording the decrease in absorbance intensity at 378 nm (λ_{max} of ADPA).[25−28] Typically, 150 μL of ADPA (5.5 mmol L^{-1}) was added into 3 mL aqueous solution of Au/SiO_2/HA, Pt/SiO_2/HA, SiO_2/HA, or free HA. The solutions were irradiated by a 470 nm light-emitting diode (LED, 25 mW), and their UV−vis spectra after irradiation were recorded by measuring the decrease in absorbance intensity at 378 nm every 30 s.

HeLa cells were cultured in the DMEM medium supplemented with 10% FCS. Cultures were incubated at 37 °C in a humidified atmosphere containing 5% CO_2. For nanoparticle uptake, cells (with about 50% confluence) in a 6-well plate suspension in the medium was combined with Au/SiO_2/HA, Pt/SiO_2/HA, SiO_2/HA, or free HA dispersion and incubated in incubator (37 °C, 5% CO_2) for 4 h. After incubation, the plates were rinsed with sterile phosphate-buffered saline (PBS), and fresh serum-free medium was replaced at a volume of 1 mL/plate. The cells were then directly imaged under a fluorescence microscope.

Chromatin condensation was detected by nuclear staining with Hoechst 33342. After treatment with Au/SiO_2/HA, Pt/SiO_2/HA, SiO_2/HA, and free HA for 4 h and irradiation by light, the cells were incubated overnight. Then, the cells were treated with Hoechst 33342 (25 μg mL^{-1}) and put back into the incubator. Fifteen minutes later, the cells were washed with sterile PBS for three times and the nuclear morphology changes were observed under fluorescence microscope.

For studying cell viability, cells (with about 80% confluence) in a 96-well plate suspension in the medium was treated with Au/SiO_2/HA5, Pt/SiO_2/HA, SiO_2/HA, and free HA, with the same amount of HA (5 μM), and incubated for 4 h. Next, the cells were rinsed three times with sterile PBS. 0.1 mL of fresh serum-free medium was added, and the plates were immediately exposed to 470 nm LED for 1 min. The plates were then returned to the incubator for 24 h. Cell viability was estimated by MTT assay and the absorbance of the formazan solution was measured at 560 and 650 nm using a Sunrise Plus plate reader (Tecan).[29]

RESULTS AND DISCUSSION

In the HA-embedding process using the conventional sol−gel silica preparation method, the amino group of APMDS was

Scheme 2. Ha Encapsulation Scheme of Pt- or Au-Doped SiO_2/HA

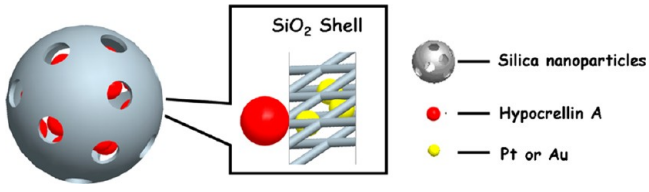

indispensable as reported by Kopelman.[26] Use of an amine derivative of oxysilane helped to keep HA inside the matrix, which is probably because of the intermolecular hydrogen bonding between the hydroxyl and carbonyl groups of HA and amine groups on APMDS, which was also proved by our previous studies. This intermolecular hydrogen bonding was critical to ensure that HA molecules can be embedded into the silica nanocarrier during the hydrolysis and polyreaction process of APMDS that followed; and similarly, Au(III) or Pt(IV) was doped into the silica structure driving for the

dx.doi.org/10.1021/jp305137j | J. Phys. Chem. B 2012, 116, 12744−12749

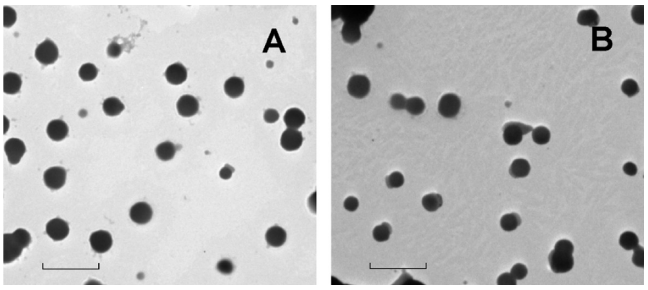

Figure 1. TEM image of $Au/SiO_2/HA$ (A) and $Pt/SiO_2/HA$ (B) (bar = 200 nm).

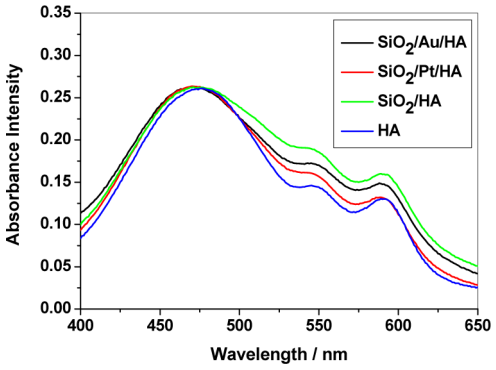

Figure 2. UV−vis spectra of HA, SiO_2/HA, $Au/SiO_2/HA$, and $Pt/SiO_2/HA$.

interaction between the heavy metal ions and amine groups on APMDS, simultaneously.

The initial endeavor of introducing Pt(IV) or Au(III) to SiO_2/HA, by simultaneously mixing HA, H_2PtCl_6 (or $HAuCl_4$), APMDS, and ammonia in methanol, was unsuccessful. This was evidenced by the reaction system which was muddy after reaction for 4 h. It turned out that adding H_2PtCl_6 (or $HAuCl_4$) after mixing HA, APMDS, and ammonia in methanol for 30 min, which is probably because Pt and Au can interact with HA and form Pt(IV)−HA or Au(III)−HA complex and such complexes possess polymer-like structures,[30] which was not propitious for the SN encapsulation process. On the contrary, if we add H_2PtCl_6 or $HAuCl_4$ after mixing HA, APMDS and ammonia in methanol for a long time, such as 4 h, the photodynamic activity of $Pt/SiO_2/HA$ and $Au/SiO_2/HA$ was much lower comparing with the samples prepared for 30 min. The above results indicated that if the position of Pt(IV) or

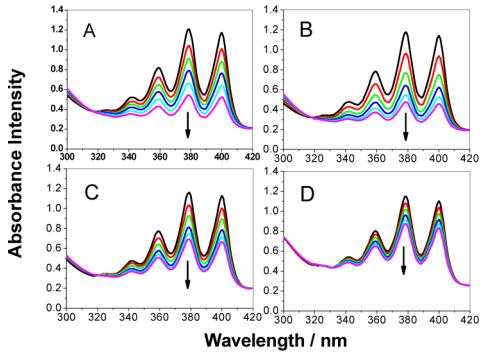

Figure 4. Absorption spectra of ADPA in $Au/SiO_2/HA$ (A), $Pt/SiO_2/HA$ (B), SiO_2/HA (C), and HA (D) systems were irradiated for 0, 30, 60, 90, 120, and 150 s.

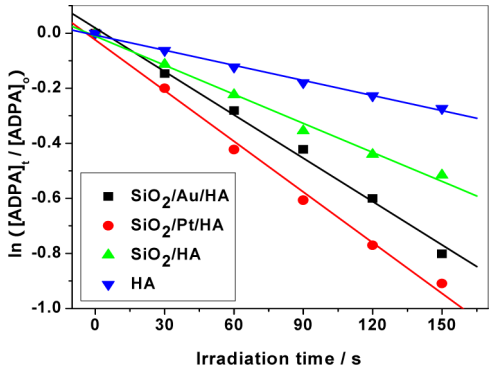

Figure 5. Reaction rate constant with ADPA by HA, SiO_2/HA, $Au/SiO_2/HA$, and $Pt/SiO_2/HA$.

Au(III) inside the SiO_2 shell were too far from HA molecule, the doped heavy metals cannot effectively improve the ISC process of HA (Scheme 2).

The typical TEM images of $Au/SiO_2/HA$ (A) and $Pt/SiO_2/HA$ (B) are shown in Figure 1. The particles are spherical and DLS measurements (Figure S5 in the Supporting Information) showed that the size distributions of $Au/HA/SiO_2$ and $Pt/HA/SiO_2$ are 99.26 ± 34.35 and 101.73 ± 37.30 nm, separately. The final size of these particles is important because the lifetime of $^1O_2$ in aqueous media is in the microseconds regime, during which interval it can diffuse over a mean radial distances of at least 100 nm; using eq 1

$$F = \sqrt{6D\tau} \quad (1)$$

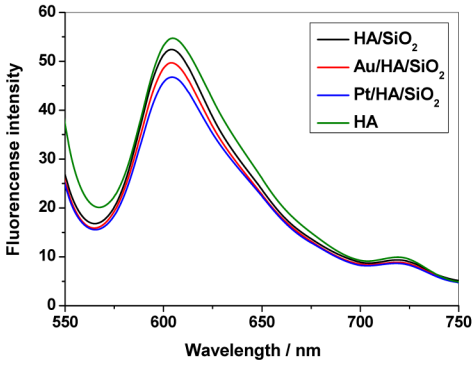

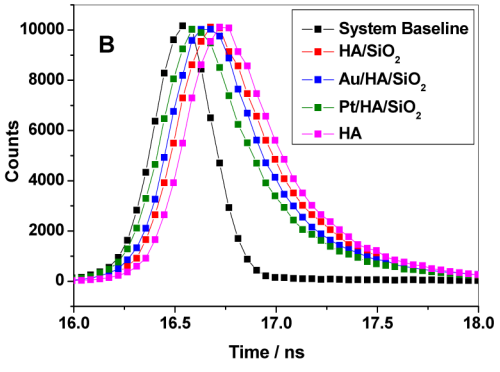

Figure 3. (A, left) Fluorescence spectra of SiO_2/HA, $SiO_2/Pt/HA$, $SiO_2/Au/HA$, and free HA. Ex = 480 nm; slit 5 nm, 5 nm; (B, right) fluorescence decays of SiO_2/HA, $SiO_2/Pt/HA$, $SiO_2/Au/HA$, and free HA.

dx.doi.org/10.1021/jp305137j | J. Phys. Chem. B 2012, 116, 12744−12749

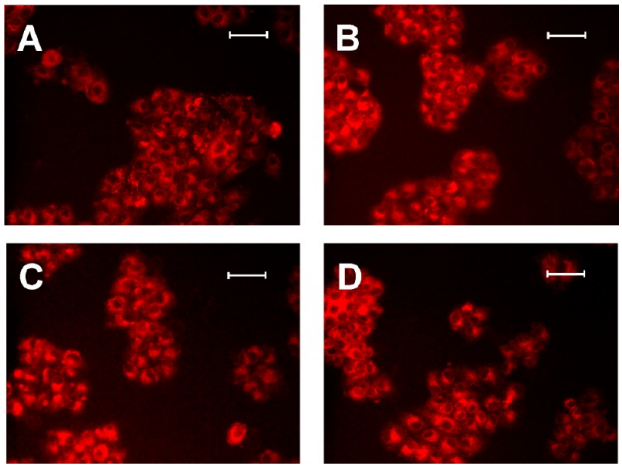

Figure 6. Fluorescence images of HeLa cells incubated with HA (A), SiO_2/HA (B), Au/SiO_2/HA (C), and Pt/SiO_2/HA (D), imaged after 4 h of incubation in serum-free media (bar = 200 μm).

where F is the mean radial displacement in time τ (=1 μs) with a diffusion coefficient; the value of D was 2×10^{-5} cm^2 s^{-1}.

The absorption spectra of HA, SiO_2/HA, Au/SiO_2/HA and Pt/SiO_2/HA are similar (Figure 2), indicating no changes in the HA chromophore upon entrapment inside nanoparticles.[25] This also demonstrates that Pt(IV) and Au(III) can be introduced without diminishing the advantageous absorption characteristics of HA.[14]

To avoid the fluorescence being affected by water, the fluorescence spectra and time-resolved fluorescence measurements of HA, SiO_2/HA, Au/SiO_2/HA, and Pt/SiO_2/HA were carried out in methanol. As showed in Figure 3A, the fluorescence spectra of HA, SiO_2/HA, Au/SiO_2/HA, and Pt/SiO_2/HA, with the same amount of HA, exhibited typical HA fluorescence peaking at about 604 nm. However, it is clearly seen that the fluorescence intensity is significantly reduced in Au/SiO_2/HA and Pt/SiO_2/HA with respect to that in SiO_2/HA. To further confirm that there is heavy atom effect between HA molecules and Pt(IV) or Au(III), time-resolved fluorescence experiments were conducted. Time-resolved fluorescence measurements examine fluorescence decay profiles and can provide evidence of the interaction between HA and heavy metal atoms.[12] Figure 3B shows the fluorescence decay curve of SiO_2/HA, SiO_2/Pt/HA, SiO_2/Au/HA, and free HA. All of the data were fitted using a reconvolution method of the instrument response function (IRF) producing χ^2 (chi squared) fitting values of 1−1.40. The average lifetimes of SiO_2/HA, SiO_2/Pt/HA, SiO_2/Au/HA, and free HA were 1.27 ns (χ^2 = 1.24), 0.90 ns (χ^2 = 1.15), 1.09 ns (χ^2 = 1.34), and 1.32 ns (χ^2 = 1.21), separately. The decrease in fluorescence intensity and lifetime of HA entrapped in Au/SiO_2 and Pt/SiO_2 in a comparison with those of HA in SiO_2 can be caused by the presence of abundant Au(III) or Pt(IV) ions in close proximity to the HA molecules. The ratio between Au(III) or Pt(IV) ions and HA is about 2, according to the feeding amounts. This implies that molecularly dispersed HA molecules in the Au(III)- or Pt(IV)-rich regions within their doped SiO_2 nanoparticles are surrounded with enough Au(III) or Pt(IV), which can enhance spin−orbit coupling and, correspondingly, there is an increase in the probability of the ISC. In this case, with an increase in population of the triplet level of the HA (^{3}HA*), an increase in $^1O_2$ sensitization may also occur,[11,12,14,31] which can further support that the intraparticle external heavy-atom effect does take place in the Au(III)- or Pt(IV)-doped SiO_2 nanoparticles.

We confirmed singlet oxygen generation by a chemical method as described before using the ADPA as a detector. Figure 4 shows the decrease in absorbance intensity at 378 nm (λ_{max} of ADPA), in different samples (HA, SiO_2/HA, Au/SiO_2/HA, or Pt/SiO_2/HA), as a function of the time of light exposure, which indicates that the amount of singlet oxygen production increased when samples were irradiated for a longer time.

The following equations are tailored specifically to the system we are dealing with, in which a $^1O_2$ detector (i.e., ADPA) and a sensitizer (i.e., HA) are irradiated together in a solution. Hypothetically, the following processes may take place (eqs 2−5):[26,27]

$$HA + H\nu \rightarrow HA^* \qquad I^{abs} \tag{2}$$

$$HA^* + {}^3O_2 \rightarrow HA + {}^1O_2 \qquad k \tag{3}$$

$$ADPA + {}^1O_2 \rightarrow ADPAO_2 \qquad k_c \tag{4}$$

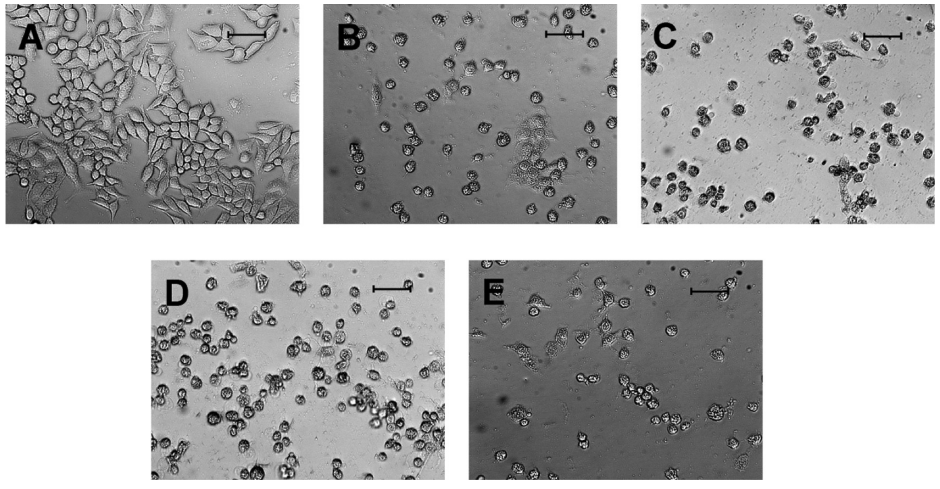

Figure 7. Microscopic images of common cells (A) and the HeLa cells treated with HA (B), Au/SiO_2/HA (C), Pt/SiO_2/HA (D), and SiO_2/HA (E) with the drug concentration of 5 μM after irradiation (bar = 200 μm).

dx.doi.org/10.1021/jp305137j | J. Phys. Chem. B 2012, 116, 12744−12749

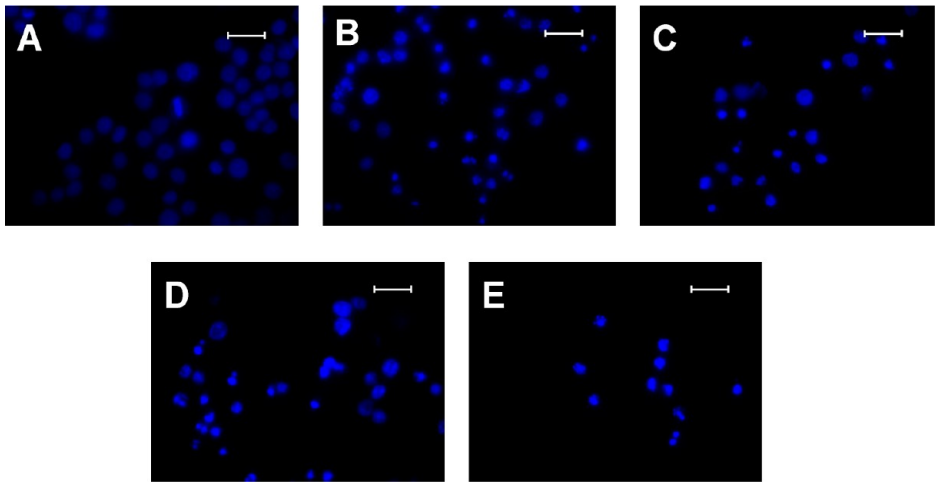

Figure 8. Microscopic images of HeLa cells nuclear morphology marked using Hoechst 33342 of common cells (A) and the HeLa cells treated with HA (B), Au/SiO_2/HA (C), Pt/SiO_2/HA (D), and SiO_2/HA (E) with the drug concentration of 5 μM after irradiation (bar = 100 μm).

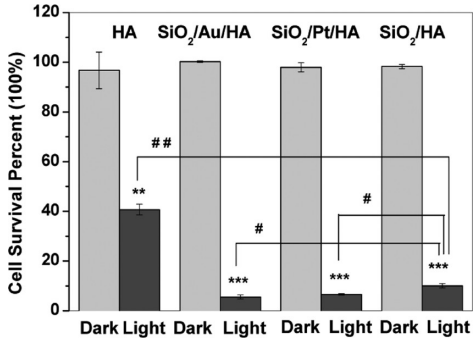

Figure 9. Comparative in vitro light-induced toxicity of HA, SiO_2/HA, Au/SiO_2/HA, and Pt/SiO_2/HA at the same experimental condition (5 μM, irradiation by 470 nm LED) (**, $p < 0.01$ vs control; ***, $p < 0.001$ vs control; control = cells were treated with drug but not irradiated by light; #, $p < 0.01$ HA vs SiO_2/HA, Au/SiO_2/HA, and Pt/SiO_2/HA; ##, $p < 0.05$ Pt/SiO_2/HA or Au/SiO_2/HA vs SiO_2/HA).

$$^1O_2 \rightarrow {}^3O_2 \qquad k_d \tag{5}$$

Here k is the rate constant for the quenching of excited HA by $^3O_2$ to produce $^1O_2$; k_c is the rate constant of chemical quenching of $^1O_2$ in the presence of ADPA; furthermore, $^1O_2$ also decays to the ground state by energy transfer to the solvent or to other species in solution, with a rate constant k_d. A rough estimation of the rate constant for the chemical quenching of ADPA by $^1O_2$ can be obtained using a simplification in which [$^1O_2$] is independent of [ADPA]. According to eq 3, the loss of ADPA in reaction, with $^1O_2$ is given by

$$-\mathrm{d}[\mathrm{ADPA}]/\mathrm{d}t = k_c[\mathrm{ADPA}][^1O_2] = k[\mathrm{ADPA}] \tag{6}$$

where

$$k = k_c[^1O_2]$$

Thus, the decay of [ADPA] follows first-order kinetics:

$$[\mathrm{ADPA}]_t = [\mathrm{ADPA}]_0 \exp(-kt) \tag{7}$$

$$\ln([\mathrm{ADPA}]_t/[\mathrm{ADPA}]_0) = -kt \tag{8}$$

After the data were plotted as $-\ln[\mathrm{ADPA}]_t/[\mathrm{ADPA}]_0$ versus irradiation time t, straight lines were obtained for the sensitizers, and the slope for each sample was obtained after fitting with a linear function, as shown in Figure 5. The exact reaction rate constant of $^1O_2$ for Au/SiO_2/HA, Pt/SiO_2/HA, SiO_2/HA, and HA is shown to be 5.25×10^{-3} ($R = 0.997$), 6.14×10^{-3} ($R = 0.997$), 3.52×10^{-3} ($R = 0.996$), and 1.83×10^{-3} ($R = 0.998$), respectively.

The above results indicate that after encapsulation inside the silica nanoparticles, the $^1O_2$ generation efficiency of HA is greatly improved, possibly because of the increased fluorescence intensity and light stability in water due to the protection effect of SN to HA (Supporting Information, Figure S6). Besides, the intraparticle external heavy atom effect significantly enhances the $^1O_2$ generation efficiency of the encapsulated HA with respect to that in SiO_2/HA, which would result in enhanced photoinduced anticancer efficacy of Pt/SiO_2/HA and Au/SiO_2/HA.

Fluorescence imaging was used to determine whether the nanoparticles were taken up by tumor cells. The fluorescence images of HA (Figure 6A), SiO_2/HA (Figure 6B), Au/SiO_2/HA (Figure 6C), or Pt/SiO_2/HA (Figure 6D) treated HeLa cells showed significant intracellular staining in the cytoplasm, indicating accumulation of samples, indicating they all can be active taken up by cancer cells. Besides, the cells were viable in the dark even after 24 h of staining, indicating low dark toxicity from the particles.

Furthermore, light irradiation of the drug-free cells did not cause any significant change in cell morphology and activity (Figure 7A). On the contrary, drastic changes in the morphology of HeLa cells that were treated overnight with Au/SiO_2/HA (Figure 7B), Pt/SiO_2/HA (Figure 7C), SiO_2/HA (Figure 7D), or HA (Figure 7E) and 15 min of irradiation were observed, and the activity of these cells was greatly decreased.

In addition, cells were stained with Hoechst 33342 to identify the photoinduced chromatin damage of the cells. The chromatin fluorescence of the cells that were only treated with drug or irradiation stained dimly and occupied the majority of the cell (Figure 8A). In contrast, the cells treated with HA (Figure 8B), Au/SiO_2/HA (Figure 8C), Pt/SiO_2/HA (Figure 8D), or SiO_2/HA (Figure 8E) and irradiation showed obvious morphology changes, including nuclear shrinkage, chromatin condensation, and fragmentation.

Figure 9 showed the cell survival percentage after treating HeLa cells with Au/SiO_2/HA, Pt/SiO_2/HA, SiO_2/HA, or HA and irradiation. The cell survival percents of Au/SiO_2/HA, Pt/

SiO_2/HA, SiO_2/HA, or HA treated cells without irradiation were 99.24%, 97.96%, 98.29%, and 96.75%, separately. In comparison all samples exhibited much less toxicity in dark; significant cell death can be observed for Au/SiO_2/HA, Pt/SiO_2/HA, SiO_2/HA particles, or HA and irradiation, and their cancer cell survival percents were 5.53%, 6.56%, 10.04%, and 40.71%, separately. The data show that HA-encapsulated nanoparticles are more effective for killing tumor cells in vitro by light exposure. Comparative studies with Pt- or Au-doped and nondoped particles indicated that the intraparticle external heavy atom effect on the encapsulated photosensitizer molecules significantly enhances the efficiency of the in vitro PDT efficacy.

CONCLUSIONS

Here, we present the first example of Pt(IV)- or Au(III)-doped silica nanoparticles formulation for PDT, in which the intraparticle external heavy atom effect on the encapsulated PS molecules significantly enhances the efficiency of $^1O_2$ generation, and thereby, the in vitro PDT efficacy. All these results showed that this technology is effective in enhancing the phototoxic effect of photosensitizers and have great potential application in the drug delivery system exploitation in PDT.

ASSOCIATED CONTENT

Supporting Information

Molecular structure of hypocrellin A; fluorescence quenching efficacies; structure scheme of HA-embedded silica nanoparticles; cell viability experiments with SiO_2, Au/SiO_2, and Pt/SiO_2 and laser irradiation for the same amount of time; dynamic light scattering patterns; and fluorescence spectra of HA and SiO_2/HA in water. This material is available free of charge via the Internet at http://pubs.acs.org.

AUTHOR INFORMATION

Corresponding Author

*Tel.: +86 25 83598359 (J.H.Z.); +86-25-83271383 (B.Y.Y.). Fax: +86 25 83598359 (J.H.Z.); +86-25-85391042 (B.Y.Y.). E-mail: zhoujiahong@njnu.edu.cn (J.H.Z.); boyangyu59@163.com (B.Y.Y.).

Notes

The authors declare no competing financial interest.

ACKNOWLEDGMENTS

This work was supported by the National Natural Science Foundation of China (20973093), the Natural Science Foundation of Jiangsu Higher Education Institutions of China (10KJB150008), the Priority Academic Program Development of Jiangsu Higher Education Institutions (PAPD), and the Scientific Research Foundation of Nanjing Normal University (No. 2011103XG0249).

REFERENCES

(1) Kastle, M.; Grimm, S.; Nagel, R.; Breusing, N.; Grune, T. *Free Radical Biol. Med.* **2011**, *50*, 305−312.
(2) Charron, G.; Stuchinskaya, T.; Edwards, D. R.; Russell, D. A.; Nann, T. *J. Phys. Chem. C* **2012**, *116*, 9334−9342.
(3) Hirakawa, K.; Hirano, T.; Nishimura, Y.; Arai, T.; Nosaka, Y. *J. Phys. Chem. B* **2012**, *116*, 3037−3044.
(4) Cheng, Y.; Meyers, J. D.; Broome, A. M.; Kenney, M. E.; Basilion, J. P.; Burda, C. *J. Am. Chem. Soc.* **2011**, *133*, 2583−2519.
(5) Zhang, Y.; Song, L. M.; Xie, J.; Qiu, H. X.; Gu, Y.; Zhao, J. Q. *Photochem. Photobiol.* **2010**, *86*, 667−672.
(6) Zhou, J. H.; Zhou, L.; Dong, C.; Feng, Y. Y.; Wei, S. H.; Shen, J.; Wang, X. S. *Mater. Lett.* **2008**, *62*, 2910−2913.
(7) Zhou, L.; Dong, C.; Wei, S. H.; Feng, Y. Y.; Zhou, J. H.; Liu, J. H. *Mater. Lett.* **2009**, *63*, 1683−1685.
(8) Zhou, L.; Liu, J. H.; Ma, F.; Wei, S. H.; Feng, Y. Y.; Zhou, J. H.; Yu, B. Y.; Shen, J. *Biomed. Microdev.* **2010**, *12*, 655−663.
(9) Zhou, L.; Liu, J. H.; Zhang, J.; Wei, S. H.; Feng, Y. Y.; Zhou, J. H.; Yu, B. Y.; Shen. *J. Int. J. Pharm.* **2010**, *386*, 131−137.
(10) Law, W. C.; Yong, K. T.; Roy, I.; Xu, G.; Ding, H.; Bergey, E. J.; Zeng, H.; Prasad, P. N. *J. Phys. Chem. C* **2008**, *112*, 7972−7977.
(11) Lim, C. K.; Shin, J.; Lee, Y. D.; Kim, J.; Park, H.; Kwon, I. C.; Kim, S. *Small* **2011**, *7*, 112−118.
(12) Kim, S.; Ohulchanskyy, T. Y.; Bharali, D.; Chen, Y. H.; Pandey, R. K.; Prasad, P. N. *J. Phys. Chem. C* **2009**, *113*, 12641−12644.
(13) Mohamed, A. A.; Rawasgdeg-Omary, M. A.; Omary, M. A.; Fackler, J. P. *Dalton Trans.* **2005**, *15*, 2597−2602.
(14) Gorman, A.; Killoran, J.; O'Shea, C.; Kenna, T.; Gallagher, W. M.; O'Shea, D. F. *J. Am. Chem. Soc.* **2004**, *126*, 10619−10631.
(15) Knyukshto, V. N.; Shulga, A. M.; Sagun, E. I.; Zenkevich, E. I. *Opt. Spectrosc.* **2006**, *100*, 590−601.
(16) Drzewiecka-Matuszek, A.; Skalna, A.; Karocki, A.; Stochel, G.; Fiedor, L. *J. Biol. Inorg. Chem.* **2005**, *10*, 453−462.
(17) McGlynn, S. P.; Azumi, T.; Kasha, M. *J. Chem. Phys.* **1964**, *40*, 507−515.
(18) Kasha, M. *Acta Phys. Pol. A* **1987**, *71*, 661−670.
(19) Kasha, M.; Khan, A. U. *Ann. N.Y. Acad. Sci.* **1970**, *171*, 5−23.
(20) Obata, M.; Hirohara, S.; Tanaka, R.; Kinoshita, I.; Ohkubo, K.; Fukuzumi, S.; Tanihara, M.; Yano, S. *J. Med. Chem.* **2009**, *52*, 2747−2753.
(21) Engelmann, F. M.; Mayer, I.; Araki, K.; Toma, H. E.; Baptista, M. S.; Maeda, H.; Osuka, A.; Furuta, H. *J. Photochem. Photobiol., C* **2004**, *163*, 403−411.
(22) Wang, Y.; He, Q. Y.; Sun, R. W. Y.; Che, C. M.; Chiu, J. F. *Cancer Res.* **2005**, *65*, 11553−11564.
(23) Janczyk, A.; Wolnicka-Gtubisz, A.; Urbanska, K.; Kisch, H.; Stochel, G.; Macyk, W. *Free Radical Biol. Med.* **2008**, *44*, 1120−1130.
(24) Petit, L.; Griffin, J.; Carlie, N.; Jubera, V.; Garcia, M.; Hernandez, F. E.; Richardson, K. *Mater. Lett.* **2007**, *61*, 2879−2882.
(25) Roy, I.; Ohulchanskyy, T. Y.; Pudavar, H. E.; Bergey, E. J.; Oseroff, A. R.; Morgan, J.; Dougherty, T. J.; Prasad, P. N. *J. Am. Chem. Soc.* **2003**, *125*, 7860−7856.
(26) Yan, F.; Kopelman, R. *Photochem. Photobiol.* **2003**, *78*, 587−591.
(27) Tang, W.; Xu, H.; Kopelman, R.; Philbert, M. A. *Photochem. Photobiol.* **2005**, *81*, 242−249.
(28) Zhou, L.; Ning, Y. W.; Wei, S. H.; Feng, Y. Y.; Zhou, J. H.; Yu, B. Y.; Shen, J. *J. Mater. Sci.—Mater. Med.* **2010**, *21*, 2095−2101.
(29) Gao, J. H.; Liang, G. L.; Zhang, B.; Kuang, Y.; Zhang, X. X.; Xu, B. *J. Am. Chem. Soc.* **2007**, *129*, 1428−1433.
(30) Zeng, Z. H.; Zhou, J. H.; Zhang, Y.; Qiao, R.; Xia, S. Q.; Chen, J. R.; Wang, X. S.; Zhang, B. W. *J. Phys. Chem. B* **2007**, *111*, 2688−2696.
(31) Rae, M.; Perez-Balderas, F.; Baleizao, C.; Fedorov, A.; Cavaleiro, J. A. S.; Tome, A. C.; Berberan-Santos, M. N. *J. Phys. Chem. B* **2006**, *110*, 12809−12814.